Zero-bias conductance dip and phonon features in the superconductor density of states observed on tantalum- and niobium-based tunneling junctions

Artur Hahn, Horst Ekrut, and Michael Westphal*
Institut für Werkstoffe der Elektrotechnik, Ruhr-Universität Bochum, Germany
(Received 18 August 1981)

From a large number of $T-T$-oxide$-$Ag tunneling junctions, with T=Ta and Nb, an empirical correlation was observed between the slope S of the normal conductance-versus-voltage characteristics and the strength of the phonon-induced features of the superconductor density of states. This correlation allows for a tentative extrapolation to the bulk tantalum density of states which, when inverted according to the Rowell-McMillan scheme, leads to parameters ($\lambda=0.80$, $\mu^*=0.15$) which deviate markedly from values accepted hitherto and stronger high-energy (longitudinal phonon) contributions to $\alpha^2F(\omega)$. For niobium, high-energy contributions to $\alpha^2F(\omega)$ stronger than recently assumed are highly probable. The slope S is governed by a zero-bias conductance dip. This anomaly as well as the nonideal features of the tunneling density of states in the superconducting state are attributed to a metal-semiconductor transition layer between the superconductor and its oxide with spatial extent of 3$-$10 Å, and at least 10 Å in the tantalum and niobium cases, respectively.

I. INTRODUCTION

Experimental results on the tunneling density of states of superconductors often deviate from theoretical expectation, leading to unreasonably low or even negative values of the Coulomb pseudopotential μ^* when formally evaluated by inverting the Eliashberg gap equations[1] according to the numerical program developed by McMillan and Rowell.[2] Particularly, this is true for niobium[3–7] and high-T_c niobium compounds, e.g., Nb_3Sn.[8]

Several authors[9] recently have accounted for these deviations in terms of a proximity theory developed by Arnold.[10] While in some of these cases a normal metallic proximity layer was assumed to lie on the superconducting metal surface beneath the insulating oxide, in other cases thin Al overlayers were deliberately evaporated and partly oxidized, a thin metallic Al proximity layer remaining beneath the oxide.

Here we report measurements on a large number of Nb$-$Nb-oxide$-$Ag and Ta$-$Ta-oxide$-$Ag tunneling junctions from which we obtained a broad variety of results on the tunneling density of states corresponding to varying degrees of deviation from ideal behavior. In Sec. IV A we shall discuss the tantalum results in terms of the Arnold theory. Our main interest, however, is in a correlation we observed between the strength of the phonon structures and the slope S of the normal conductance-versus-voltage characteristics at low voltage (about 20 mV). In Sec. II we present observations indicating that this slope is largely determined by a zero-bias anomaly consisting of a broad conductance dip. While this correlation is in itself an important result (to be discussed in Sec. IV B), in the following sections, S is used as a strictly phenomenological quantity to qualify the nonideality of junctions and to extrapolate to an "ideal" junction in the tantalum case.

II. SAMPLES AND PREVIOUS RESULTS

In this investigation we are concerned with the low-bias normal and superconducting properties of a great number of junctions. These are the same junctions the high-voltage background conductance of which was described in a previous paper,[11] hereafter referred to as paper I. Hence we refer to this paper for details of the junction preparation, and here only mention that the tunneling junctions were built up on ultrahigh vacuum (UHV) molten spheres of niobium and tantalum, oxidized either thermally in air or in an O_2 plasma, and counter-contacted with silver.

In the course of another parallel investigation,[12] part of the niobium samples were deliberately

doped at temperatures of some hundred degrees Celsius, with oxygen doses in the 3–7 langmuir range, before air oxidation at room temperature was performed.

From the background conductance as given in paper I, high asymmetric barriers were deduced for the thermally air-oxidized samples while the plasma-oxidized samples, according to their background conductance, obviously developed low poor-quality tunneling barriers. Corresponding observations of "high" and "low" quality also result for the tunneling characteristics in the superconducting state as will be seen in the following.

As stated in paper I, for high-quality junctions, a rather symmetric zero-bias anomaly was observed below 50 mV, consisting of a 10–25 % conductivity dip, generally larger for niobium than for tantalum. In Fig. 1(a), curve *A*, an example is given for niobium along with the low-bias characteristics of the same sample in the superconducting state [Fig. 1(b)]. Despite its relatively small contribution to the normalized conductance in the normal state,

$$\hat{G}=\frac{\left[\frac{dJ}{dU}\right]_n(U)}{\left[\frac{dJ}{dU}\right]_n(U=0)}, \tag{1}$$

the zero-bias anomaly constitutes the main contribution to the slope,

$$S(U)=\frac{d\hat{G}}{d\,|\,U\,|}, \tag{2}$$

at, say, 20–30 mV, on account of its strong variation with voltage. Hence, the quantity *S*, evaluated in this voltage range, seems a suitable empirical measure of the zero-bias anomaly.

On the other hand, poor-quality junctions showed strong variations of normalized conductance with voltage over the whole measurable range of voltage (in most cases only 200–500 mV) and a separation into "background" and "zero-bias-anomaly" contributions was no longer possible. In particular, variation at a bias below 50 mV was appreciably stronger than the variation, due to the zero-bias anomaly for the high-quality junctions.

An example for a "low-quality" characteristic obtained on a niobium junction is also given in Fig. 1(a) (curve *B*). In comparing curves *A* and *B* one is intuitively tempted to attribute all of the low-quality-junction conductance to a "giant" zero-bias anomaly. Postponing a discussion of the physics underlying the zero-bias anomaly to Sec. IV B, in the following we use the easily measurable quantity *S* as a parameter to represent the characteristic superconducting phonon structures and shall show, as a main result, that phonon structures are weakened with increasing *S*.

Before presenting and discussing results some remarks should be made concerning the way these results were obtained. In fact, they were not planned to be presented in this form, but rather the results were to constitute a by-product of two different investigations, one concerning the high-field gapless density of states of pure and dirty niobium in the vortex phase,[12] and one concerning background conductance and barrier shape (paper I and Ref. 13). Although interest was mainly in the gap region in the former case and in the normal background conductance on the 1-V scale in the latter case, phonon structures in the superconducting state characteristics in many cases were routinely recorded for completeness. Workers in the field will recognize that there was some hope behind

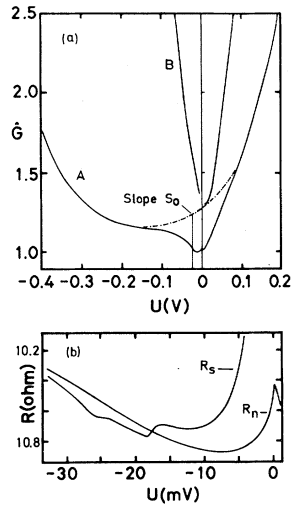

FIG. 1. (a) Conductance vs voltage for two different Nb-oxide-Ag junctions at 1.5 K. Superconductivity suppressed by magnetic field. *A* represents the "high-quality" junction, showing asymmetric conductance and the "zero-bias anomaly" consisting in a conductance dip below 50 mV. The small conductance peak in the millivolts regime constitutes another "zero-bias anomaly" which is due to magnetic impurity scattering and is not discussed in this paper. *B* represents the "low-quality" junction. Scale shifted upwards by +0.3 units. (b) Differential resistance in the normal and superconducting state of junction *A*. $T=1.5$ K.

these investigations to improve $a^2F(\omega)$, λ, and μ^* values for niobium, for which even the best values deviated markedly from theoretical expectation as mentioned before.

While a drastic improvement of phonon structures was not achieved, we obtained a very large number of results on different samples in this manner, showing a correspondingly broad variation between "good" and "poor" results with respect to theoretical expectation. In contrast with most other investigations on tunneling junctions representing only one or a few samples, we have at our disposal results on more than 50 samples which enable us to look for systematic variations beyond statistical scattering.

The results presented here are somewhat incomplete, however, in one respect: In most cases, phonon-induced structures were measured only for positive bias in the tantalum case and only for negative bias in the niobium case, the reason simply being that different experimentalists worked with niobium and tantalum (here, by convention, we refer to the polarity of the Ta or Nb electrode relative to that of the Ag electrode). Since the slope S of the normal conductance was obtained from the same measurements, S contains a small background contribution S_0 which is positive for Ta and negative for Nb-based junctions. This fact will be considered later in discussing Figs. 3–5.

III. RESULTS

To represent the results on Ta–Ta-oxide–Ag tunneling junctions, we determined, from the measured conductance in the superconducting (s) and in the normal (n) state, the normalized tunneling density of states,

$$N_T(E)=\frac{\left[\frac{dJ}{dU}\right]_s}{\left[\frac{dJ}{dU}\right]_n}\ , \tag{3}$$

and the BCS-normalized tunneling density of states,

$$n_T(E)=N_T(E)/N_T^{\mathrm{BCS}}(E)\ , \tag{4}$$

with

$$E=eU\ , \tag{5}$$

$$N_T^{\mathrm{BCS}}(E)=\frac{E}{(E^2-\Delta_0^2)^{1/2}}\ , \tag{6}$$

and

$$\Delta_0=0.72\ \mathrm{meV}\ , \tag{7}$$

with this value given by Shen,[14] and also corresponding to values obtained in this laboratory.[4,15]

In Fig. 2, $n_T(E)$ curves are given as measured on three different junctions corresponding to different values of the slope S (20 mV) of the normal conductance-versus-voltage curve, defined in Eq. (2) and taken at $U=20$ mV.

In the following, in order to represent the gross features of characteristics like those represented in Fig. 2, we use the $n_T(E)$ values, $n_T(10)$ and $n_T(15)$, occurring, respectively, at $E=eU=10$ and 15 meV, and the minimum value $n_T^{\min}$ of $n_T(E)$, occurring at slightly varying energies E, slightly below 19 meV. The $n_T(10)$ and $n_T(15)$ values are characteristic of the nearly horizontal portions of the $n_T(E)$ curves preceding the first and second steep descents, these descents resulting from the transverse and longitudinal phonon density-of-states peaks, respectively. The amplitudes of these descents,

$$\begin{aligned}\delta n_T^{\mathrm{trans}}&=n_T(10)-n_T(15)\ ,\\ \delta n_T^{\mathrm{long}}&=n_T(15)-n_T^{\min}\ ,\end{aligned} \tag{8}$$

are also used in the following to represent different strengths of the phonon-induced structures for different samples.

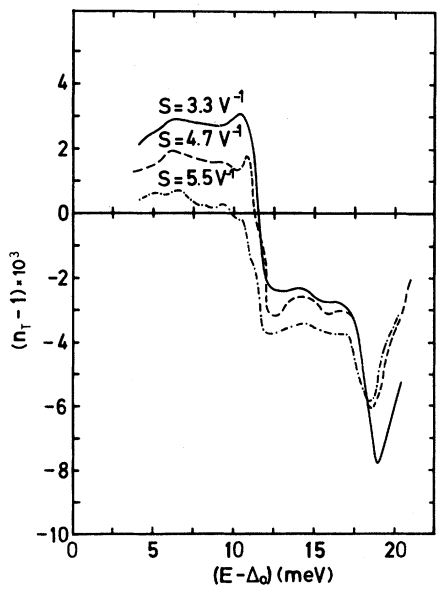

FIG. 2. BCS-normalized tunneling density of states, at $T=1.5$ K, for three different Ta-oxide–Ag junctions with different $S=S(20\ \mathrm{mV})$.

For the best Nb-oxide—Ag junctions the BCS-normalized density of states is similar to that given previously by Gärtner and one of us,[4] and later on discussed in terms of a proximity layer by Arnold *et al.*[16] Here only $\delta N_T^{\text{trans}}$ and δN_T^{long} values are represented in the following, defined as the amplitudes of the descents of N_T (not n_T) over an energy interval of 3 meV around the energies of steepest descent, dN_T/dE; these energies roughly being given by $E=eU=18$ and 25.5 meV for transverse and longitudinal phonons, respectively.

The characteristic data $n_T(10)$, $n_T(15)$, and $n_T^{\min}$ for Ta-based junctions are given as functions of S (20 mV) in Fig. 3. Samples oxidized in air and masked with Formvar outside the vacuum chamber before counter contacting (see paper I) are marked by crosses while the dots represent samples plasma oxidized in pure oxygen and *in situ* counter contacted. The δn_T and δN_T values, representing the strength of phonon features, are given in Fig. 4 for Ta, and in Fig. 5 for Nb-based junctions as functions of the slope S (evaluated for niobium junctions at $U=-25$ mV). As may be seen from these figures, these structures continuously get weaker for increasing S values. The weakening of structure is much stronger for the longitudinal than the transverse phonon structure in both the Ta and Nb cases. For niobium, the longitudinal phonon structure is no longer observable for samples plasma oxidized in pure oxygen and *in situ* counter contacted. These samples, in general, show very large S values, i.e., the strongly non-Ohmic behavior of the normal conductance.

Observing the empirical correlation between the strength of phonon-induced structures and the quantity S, one might ask which value of S corresponds to an ideal superconductor surface. Since, according to paper I, asymmetric background conductance is observed for the high-quality (low S, strong phonon features) junctions,

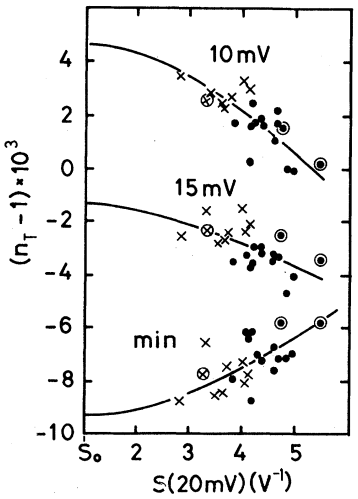

FIG. 3. BCS-normalized conductance for 23 Ta-oxide—Ag junctions at three characteristic energies represented vs S(20 mV). Crosses represent samples oxidized in air. Dots represent samples plasma-oxidized and *in situ* counter contacted. Encircled symbols represent the three junctions represented in Fig. 2. For S_0 defined at the end of Sec. III, a value 1 ± 0.5 V^{-1} was obtained from the asymmetric background conductance of several junctions, examples of which are given in paper I.

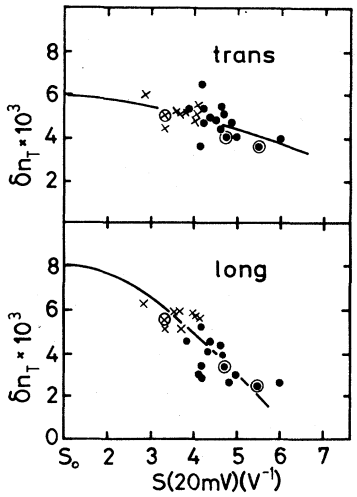

FIG. 4. The amplitudes, $\delta n_T^{\text{trans}}$ and δn_T^{long}, of the steep descent vs S(20 mV) for the Ta-oxide—Ag junctions of Fig. 3. Dots, crosses, and circles as in Fig. 3. For extrapolation to $S=S_0$ here and in Fig. 3, see Sec. IV.

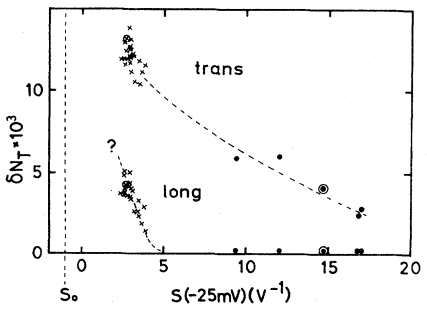

FIG. 5. The amplitudes $\delta N_T^{\text{trans}}$ and δN_T^{long} vs $S(-25$ mV) for Nb-oxide—Ag junctions. Crosses and dots as in Fig. 3. Encircled symbols represent the two junctions represented in Fig. 1. The rough value $S_0=-1\pm0.5$ V^{-1} is obtained as indicated in Fig. 1.

the value S_0 for an "ideal" junction is given by the slope of this background conductance, a rough value of which is indicated in Figs. 3–5. According to the comment concluding Sec. II, S_0 is positive for Ta and negative for Nb-based junctions.

IV. DISCUSSION

We first discuss the experimental data in terms of proximity theory, thereby treating the parameter S as a strictly phenomenological quantity which is empirically correlated with the shortcomings of superconducting characteristics. Then, an attempt is made to understand the physics of this correlation.

A. Discussion of data in terms of proximity theory

The BCS-normalized density of states as obtained for the lowest S, tantalum-based junctions is comparable with the data obtained previously by Shen,[14] and by Gärtner and one of us,[4] and, according to these investigations, is roughly consistent with the strong-coupling theory, leading typically to μ^* values slightly above 0.1 and λ between 0.7 and 0.8. The phonon structures of the lowest-S niobium junctions are also comparable in strength with the strongest structure data contained in the literature[3–7,17,18] and obtained on different systems, including aluminum-oxide barriers and metallic aluminum proximity layers. As is well known now, and was stated in one of the first papers on the subject,[3] any direct attempt to invert such data according to the McMillan and Rowells numerical program leads to unsatisfactory results; these shortcomings resulting, at least in some cases, from a normal proximity layer on the surface of the superconductor.

Examining Figs. 3–5 and, *ad hoc*, using $S-S_0$ as a measure of the influence of the proximity layer, the appreciably higher $S-S_0$ values for the niobium as compared with the tantalum junctions should be noted.

One could attempt to extrapolate phonon-induced structures to $S=S_0$ in order to obtain the characteristics of an ideal superconductor representing bulk properties. While this extrapolation seems hopeless in the niobium case (see Fig. 5), we have attempted to extrapolate the tantalum data as indicated by the curves in Figs. 3 and 4. The $n_T(10)$, $n_T(15)$, and $n_T^{\min}$ data (and, accordingly, the $\delta n_T^{\text{trans}}$ and δn_T^{long} data) are extrapolated, ambiguously postulating vanishing slopes at $S=S_0$. Moreover, we extrapolated (and partly interpolated) the entire $n_T(E)$ curve to $S=S_0$, the result being given in Fig. 6(a). Here, we again emphasize the ambiguity of this extraplation. In particular, we have no theoretical argument postulating monotonic behavior and vanishing slope at $S=S_0$ of n_T ($E=$const) as a function of S.

However, we claim that the (more or less) ambiguously extrapolated $n_T(E)$ of Fig. 6(a) represents a better approximation to the true bulk tantalum BCS-normalized density of states than do any of the directly measured nonideal $n_T(E)$ curves with $S \gtrsim 3\ \text{V}^{-1}$, including those given in the literature. This view is supported by the following analysis on the basis of Arnold's proximity theory[10] which, starting from the data of Fig. 6, leads to the observed nonideal behavior with reasonable values obtained for the thickness of the postulated proximity surface layer.

Figure 6(b) represents $\alpha^2F(\omega)$, the phonon density of states weighted by the electron-phonon interaction strength, as obtained from the proposed $n_T(E)$ by the Hubin numerical program[19] of the Rowell-McMillan inversion scheme. λ and μ^*

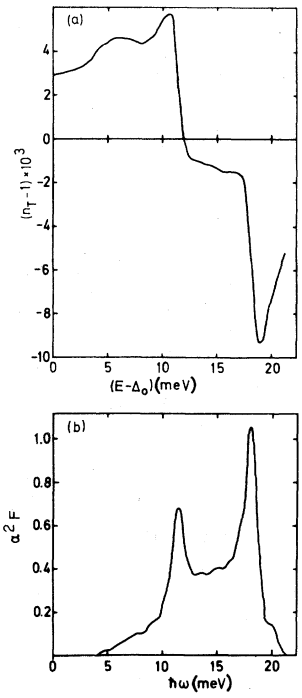

FIG. 6. BCS-normalized density of states $n_T(E)$, extrapolated to $S=S_0$, and $\alpha^2F(\omega)$ corresponding to $n_T(E)$ for tantalum ($\lambda=0.80$, $\mu^*=0.15$).

values were 0.80 and 0.15, and the calculated transition temperature was $T_c = 5.04$ K. In fact, Fig. 6(a) represents just the theoretical $n_T(E)$ corresponding strictly to $\alpha^2F(\omega)$ and μ^*. This theoretical $n_T(E)$ deviates only very slightly from the extrapolated empirical curve. It is just $\alpha^2F(\omega)$, μ^*, and the resulting energy renormalization, gap, and tunneling density of states functions $Z(E)$, $\Delta(E)$, and $n_T(E)$ that we take as the model of tantalum's bulk superconducting properties in the following analysis.

For a further discussion of the experimental curves in terms of a nonsuperconducting metallic surface layer we made use of the high-energy ($E >> |\Delta|$) limit of the Arnold proximity theory[10] for vanishing pair potential in the proximity layer, which gives for the tunneling density of states

$$N_T(E)-1=\frac{\Delta_1^2-\Delta_2^2}{2E^2}\langle e^{-xZ_2E\gamma}\cos(xZ_1E\gamma)\rangle - \frac{\Delta_1\Delta_2}{E^2}\langle e^{-xZ_2E\gamma}\sin(xZ_1E\gamma)\rangle , \tag{9}$$

with

$$\gamma=\frac{4d}{\hbar v_F} , \tag{10}$$

where v_F is the Fermi velocity, and d is the thickness of the proximity layer. We have

$$\Delta=\Delta_1+i\Delta_2 \tag{11}$$

as the pair potential in the superconductor, and

$$Z=Z_1+iZ_2 \tag{12}$$

as the energy renormalization function in the proximity layer.

Finally

$$x=(\cos\vartheta)^{-1} , \tag{13}$$

and $\langle\ \rangle$ indicates taking the mean value over the angle ϑ between quasiparticle moment and surface normal direction with suitable weighting of different ϑ according to the tunneling probability.

In the form given above, the theory was applied to experimental data by several authors. (See Refs. 7, 9, and 16–18, and additional papers quoted therein.) Occasionally, the effect of nonvanishing pair potential in the proximity layer was also included.[18] In any case, an energy-independent, purely imaginary additive contribution was assumed in the normal self energy $[1-Z(E)]E$ on account of impurity scattering in the proximity layer, which, when separately noted in formula (9), leads to an additional energy-independent factor $e^{-2xd/l}$, where the remaining term $e^{-xZ_2E\gamma}$, now describes quasiparticle damping solely by phonon excitation. l is the mean free path in the proximity layer.

An application of the full theory eventually seems possible in cases where the energy renormalization function Z of the normal layer is independently known as is assumed to be the case with thin aluminum overlayers on, e.g., Nb.[17,18] In our case of a disturbed metallic transition layer between the superconductor and its oxide, the properties of this layer are neither well known nor is this layer expected to be homogeneous as postulated by theory. Instead, as will be discussed in Sec. IV B, we think of this layer as a gradual transition region of some spatial extent, between the metal and the dielectric oxide, having a gradual change of properties.

Hence, rather than making any attempt of sophisticated parameter fitting, we study the predictions from theory in three limiting cases, the physical meaning of which is quite simple, and compare these predictions with experimental findings.

Case (A). Only energy-independent impurity scattering is assumed, formally described by

$$d/v_F\to 0,\quad d/l \text{ finite} . \tag{14}$$

This leads to an energy-independent damping of structures in $N_T(E)$:

$$N_T(E)-1=\frac{\Delta_1^2-\Delta_2^2}{2E^2}\langle e^{-2xd/l}\rangle . \tag{15}$$

Case (B). Any damping of quasiparticle excitations in the proximity layer is neglected, formally,

$$d/l\to 0,\quad Z=1 . \tag{16}$$

In this case only the phase shift over the proximity layer is effective, represented by the cosine and sine terms in Eq. (9), while damping not only by impurity scattering but also by real phonon excitations is neglected.

Case (C). While case (B) is certainly an underestimate of electron-phonon interaction in the proximity layer, an upper limit should be given by assuming for the proximity layer, the full strength of electron-phonon interaction of the bulk tantalum metal. This is our procedure in the third model calculation, case (C), given by:

$$d/l\to 0,\quad Z=Z_{\mathrm{Ta}} . \tag{17}$$

Case (A) was assumed by Wolf *et al.*[16] in the

aforementioned analysis of the data of Ref. 4. In contrast, in the very first discussions of tunneling into transition metals,[2,3,14] the observed shortcomings have been blamed on the quasiparticle damping by phonon emission, described by $\exp(-xZ_2E\gamma)$ as in case (C). As will be seen, the analysis of the tantalum data will give some answer to the question whether energy-independent [case (A)] or energy-dependent effects [cases (B) and (C)] dominate.

In the model calculations, a random distribution of ϑ over the half-sphere was assumed in taking the mean value in Eq. (9) since the k_x,k_y-conserving selection rules are not expected to apply for the electron transition from the metal to the amorphous oxide constituting the barrier.

Results are represented in Figs. 7 and 8. The BCS-normalized tunneling density of states, as calculated from the data of Fig. 6 for three different values of the parameter γ, is given in Fig. 7(b) for $Z=1$ [case (B)], and in Fig. 7(c) for $Z=Z_{\mathrm{Ta}}$ [case (C)]. γ values were chosen in order to represent roughly the experimental curves of Fig. 2, repeated in Fig. 7(a) for comparison. Comparing Figs. 7(b) and 7(c) with Fig. 7(a) we conclude that, with suitably fitted γ values, the theory is well suited to represent the characteristic variations of $n_T(E)$ when passing from high- to low-quality junctions. This is true for both assumptions $Z=1$ and $Z=Z_{\mathrm{Ta}}$, with the γ values, and hence, proximity layer thickness d, being smaller in the latter case.

In Figs. 8(c) and 8(d) we represent, as functions of γ, calculated values of $n_T(10)$, $n_T(15)$, and $n_T^{\min}$ for cases (B) and (C), respectively. For comparison, in Fig. 8(a), the experimental data of Fig. 4 are repeated. In comparing these data with the theoretical results Figs. 8(c) and 8(d) one must remember that S cannot be expected to vary *linearly* with γ (that is, the proximity layer thickness), but instead must be assumed some unknown nonlinear monotonically increasing function of γ. Hence, the different curvatures of curves in Figs. 7(a), 7(c), and 7(d) are meaningless and all that can be concluded is that the theory well represents the general tendency of experimental findings in going from high- to low-quality junctions as indicated by increasing parameter S. In particular, the calculated $\delta n_T^{\mathrm{long}}=n_T(15)-n_T^{\min}$ value decreases more quickly than $\delta n_T^{\mathrm{trans}}=n_T(10)-n_T(15)$, in accordance with experimental findings.

Assuming case (A), we obtain a quite different result which is represented in Fig. 8(b). Here, $\delta n_T^{\mathrm{trans}}$ is reduced more quickly with increasing parameter $(d/l)_{\mathrm{eff}}$ than $\delta n_T^{\mathrm{long}}$ is, in disagreement with experimental findings. Here $(d/l)_{\mathrm{eff}}$ is defined by

$$\langle e^{-2xd/l}\rangle = e^{-2(d/l)_{\mathrm{eff}}} . \tag{18}$$

In fact, disregarding the details of the theoretical model, the experimental result is characterized by a strongly energy-dependent weakening of phonon structures, the high-energy (longitudinal phonon) structure being more drastically reduced than the low-energy structure. As a consequence, the $S\rightarrow S_0$ extrapolation to an idealized tunneling density of states has led to an $\alpha^2F(\omega)$ in Fig. 6, whose longitudinal-to-transverse peak height ratio is markedly larger than previously obtained,[14,4] and

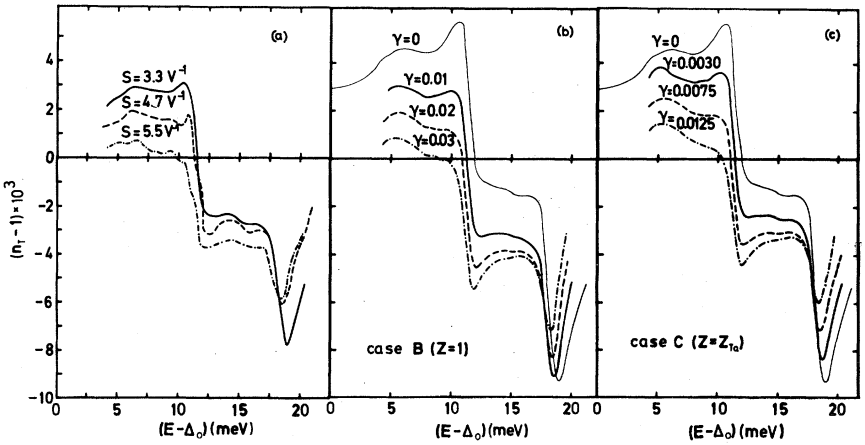

FIG. 7. (a) Experimentally determined, BCS-normalized density of states $n_T(E)$ for Ta-based junctions with different S values (see Fig. 2). (b) and (c) Theoretical $n_T(E)$ curves obtained from the bulk tantalum data of Fig. 6 for different values of parameter γ in cases (B) and (C). (See text.) γ in $(\mathrm{meV})^{-1}$.

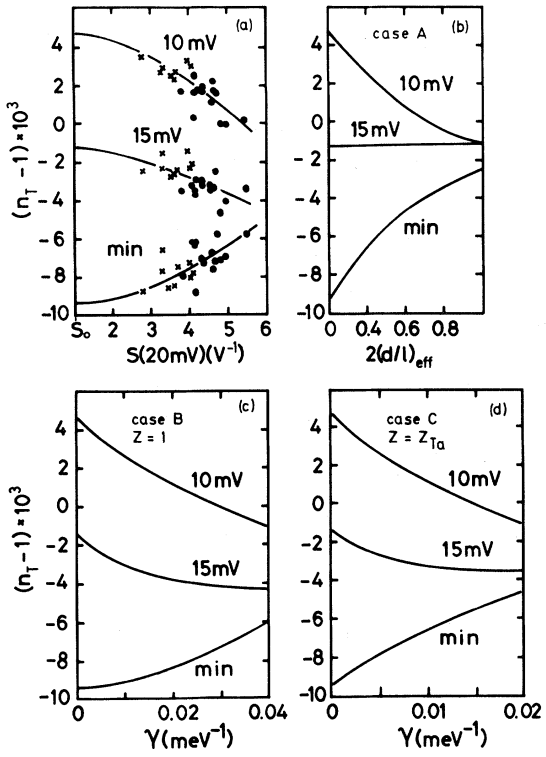

FIG. 8. BCS-normalized density of states at characteristic energies for Ta-based junctions. (a) Experimental results plotted versus $S(20\text{ mV})$. (b) Theoretical results for case (A) plotted vs $2(d/l)_{\text{eff}}$. (c) Theoretical results for case (B) plotted vs γ. (d) Theoretical results for case (C) plotted vs γ.

hence more closely resembles the $F(\omega)$ results obtained from inelastic-neutron-scattering experiments.[20] Hence, the experimental result on tantalum gives confirmation to the very first discussions[2,3] of the shortcomings of tunneling results into transition-metal superconductors in terms of an energy-dependent damping.

On the other hand, more recent discussions of the proximity effect in niobium-based junctions lead to a drastically different result, stating that dn_T/dE and, correspondingly, α^2F, as obtained by the McMillan program without considering proximity effects, are essentially reduced in amplitude, their general shape being not much affected.[7,16,18] As a consequence, $\alpha^2(\omega)$ would be assumed to be a monotonically decreasing function.

At least for thermally oxidized tantalum, our experimental result indicates different behavior. As is shown by Fig. 6, even a vanishing contribution of low-energy phonons is compatible with experiments. This would correspond to McMillan's neglect of long-wavelength transverse phonons in his model phonon density of states for niobium.[21] While in case (C) the weakening of phonon structures at high energy is due to both phase shift and damping effects, in case (B) only phase-shift effects occur. These effects play a more essential role in reducing the longitudinal phonon structure than in previous applications of the Arnold theory, because here random instead of specular transmission is assumed. This leads to destructive interference on account of different path lengths $d/\cos\vartheta$ of quasiparticles across the proximity layer. Experimentally, cases (B) and (C) cannot be distinguished on the basis of the available material.

Assuming a value for the Fermi velocity, v_F, in the proximity layer, we obtain an interval of d values from the γ values representing the experimental spectrum of characteristics. In taking $v_F=0.24\times10^8$ cm/s typical for bulk tantalum,[22] we obtain from Eq. (10) for case (B):

$$0.01\ (\text{meV})^{-1}<\gamma<0.03\ (\text{meV})^{-1}\ ,$$

$$4\ \text{Å}<d<12\ \text{Å}\ ,$$

and for case (C):

$$0.003\ (\text{meV})^{-1}<\gamma<0.0125\ (\text{meV})^{-1}\ ,$$

$$1.2\ \text{Å}<d<5\ \text{Å}\ .$$

As mentioned above, cases (B) and (C) are extreme assumptions and hence, some intermediate d values seem most probable. Hence we conclude that the tantalum-oxide-Ag junctions obtained by us have normal proximity layers between 3 and 10 Å thick, the lower value being valid for high-quality junctions. Since this is only a single monolayer we conclude that there is no chance to prepare junctions with a tunneling density of states coming closer to bulk tantalum properties than those reported up to now[14,4] and in the present investigation.

In comparing Figs. 4 and 5, one intuitively might guess from the $S-S_0$ values that the best niobium junctions correspond to the lowest-quality tantalum junctions. Hence, a proximity layer of about 10-Å spatial extent may be assumed for the highest-quality niobium junctions. An extrapolation to bulk properties seems difficult. The extrapolations which have been made until now in terms of Arnold's theory seem to depend strongly on the assumption of specular tunneling. Abandoning this assumption in favor of random tunneling might lead to markedly different results. Particularly, according to the above model calculation

for tantalum, we should expect an enhancement of the longitudinal peak in $\alpha^2F(\omega)$ in this case. In any case, direct experimental results are highly desirable on junctions with a more abrupt transition from the undisturbed metal to an insulating barrier.

B. Zero-bias anomaly

The correlation observed between the slope S of the normal conductance-versus-voltage characteristics, and weakening of phonon structures, does not seem unexpected. Large slope, i.e., strong non-Ohmic behavior of normal conductance, generally means a low mean-oxide barrier height. However, for a low barrier the transition between bulk metallic properties and dielectric properties of the oxide must be expected to be more gradual than for a high barrier where this transition may occur abruptly, typically within one atomic distance. The correlation under question has been extensively discussed along these lines in paper I and we refer to this discussion instead of repeating it here.

The question remains, why does the low-bias, non-Ohmic behavior manifest itself as a conductance dip which is well separated from the background conductance? [Examples are given in Fig. 1(a) of this paper and Fig. 4 of paper I.]

As a preliminary interpretation we attribute this anomaly to tunneling into the same degenerate metal-semiconductor transition layer between the tantalum or niobium metal and its oxide, which is responsible for the weakening of phonon structures. Zero-bias conductance dips of generally much higher amplitude than those observed here have often been reported for tunneling through Schottky barriers into a degenerate semiconductor near a Mott transition.[23] More recently, similar results have been reported for tunneling into amorphous metallic systems close to the Anderson localization limit and interpreted in terms of a density-of-states minimum.[24,25] Although the corresponding theory is not yet developed for the spatially inhomogeneous case of a transition region between a pure metal and its amorphous oxide, the assumption seems reasonable that a weak version of the conductance minimum is also observed in this case. Assuming this, one must expect the intensity of the zero-bias anomaly, as measured by the slope $S-S_0$ to be correlated with the spatial extension of the transition region.

Preliminary results on the temperature dependence of the conductance dip between 1.5 and 290 K clearly exclude an alternative explanation in terms of inelastic-tunneling contributions which lead to conductance minima in other cases.[26] In particular, the temperature dependence is too strong to be accounted for by thermal smearing of the Fermi distribution function. While such strong temperature dependence has been observed in the semiconductor case,[23] both experimental and theoretical analysis of the temperature dependence is lacking in the amorphous metal case. Hence, the problem needs closer examination in the future.

ACKNOWLEDGMENT

Part of this work was supported by the Deutsche Forschungsgemeinschaft.

---

*Now at Vacuumschmelze Hanau.

[1]G. M. Eliashberg, Zh. Eksp. Teor. Fiz. 38, 966 (1960); 39, 1437 (1960) [Sov. Phys. — JETP 11, 696 (1960); 12, 1000 (1961)].

[2]W. L. McMillan and J. M. Rowell, in *Superconductivity*, edited by R. D. Parks (Dekker, New York, 1969), p. 561.

[3]L. Y. L. Shen, in *Superconductivity in d- and f-Band Metals*, edited by D. H. Douglass (AIP, New York, 1972), p. 31.

[4]K. Gärtner and A. Hahn, Z. Naturforsch. 31A, 858 (1976).

[5]J. Bostock, K. H. Lo, W. N. Cheung, V. Diadiuk, and M. L. A. Mac Vicar, in *Superconductivity in d- and f-Band Metals*, edited by D. H. Douglass (AIP, New York, 1976), p. 367.

[6]B. Robinson, T. H. Geballe, and J. M. Rowell, in *Superconductivity in d- and f-Band Metals*, edited by D. H. Douglass (AIP, New York, 1976), p. 381.

[7]J. Bostock, M. L. A. Mac Vicar, G. B. Arnold, J. Zasadzinski, and E. L. Wolf, in *Superconductivity in d- and f-Band Metals*, edited by H. Suhl and M. B. Maple (Academic, New York, 1980), p. 153.

[8]L. Y. L. Shen, Phys. Rev. Lett. 29, 1082 (1972).

[9]See, for example, E. L. Wolf, J. Zasadzinski, G. B. Arnold, D. F. Moore, J. M. Rowell, and M. R. Beasley, Phys. Rev. B 22, 1214 (1980), and references therein.

[10]C. B. Arnold, Phys. Rev. B 18, 1076 (1978).

[11]M. Brunner, H. Ekrut, and A. Hahn, J. Appl. Phys. 53, 1596 (1982); quoted as paper I.

[12]M. Westphal, Doctorial thesis, Bochum, 1979 (unpublished).

[13]H. Ekrut and A. Hahn, J. Appl. Phys. 51, 1686 (1980).

[14]L. Y. L. Shen, Phys. Rev. Lett. 24, 1104 (1970).
[15]H. Ekrut and A. Hahn (unpublished).
[16]G. B. Arnold, J. Zasadzinski, and E. L. Wolf, Phys. Lett. 69A, 136 (1978).
[17]E. L. Wolf and J. Zasadzinski, Phys. Lett. 62A, 165 (1977).
[18]E. L. Wolf, J. Zasadzinski, J. W. Osmun, and G. B. Arnold, Solid State Commun. 31, 321 (1979).
[19]W. N. Hubin, University of Illinois, Technical Report No. 182 (unpublished).
[20]A. D. B. Woods, Phys. Rev. 136, A781 (1964).
[21]W. L. McMillan, Phys. Rev. 167, 331 (1968).
[22]This value was quoted in Ref. 3 with reference to L. F. Mattheiss, Phys. Rev. B 1, 373 (1970).
[23]For example, E. L. Wolf, R. H. Wallis, and C. J. Adkins, Phys. Rev. B 12, 1603 (1975), and references therein.
[24]B. L. Altshuler and A. G. Aronov, Solid State Commun. 30, 115 (1979); with application to experiments by S. Bermon and C. K. So, Solid State Commun. 27, 723 (1978).
[25]W. L. McMillan and J. Mochel, Phys. Rev. Lett. 46, 556 (1981).
[26]J. M. Rowell, in *Tunneling Phenomena in Solids,* edited by E. Burstein and S. Lundquist (Plenum, New York, 1969), p. 385.